Bulletin of the Seismological Society of America, Vol. 92, No. 7, pp. 2659–2669, October 2002

Displacement across the Cholame Segment of the San Andreas Fault between 1855 and 1893 from Cadastral Surveys

by Eric E. Runnerstrom, Lisa B. Grant, J Ramón Arrowsmith, Dallas D. Rhodes, and Elizabeth M. Stone

Abstract Changes since 1855 in reported section-line lengths and positions of survey monuments that span the San Andreas fault (SAF) were used to measure displacement interpreted to be from the 1857 Fort Tejon earthquake in south-central California. In 1855–1856 James E. Freeman established township and range lines across the SAF between Rancho Cholame and the northern Carrizo Plain. At least 26 1-mile sections lines spanned the SAF in the area between present-day California Highways 46 and 58. Each section line was marked by monuments at the midpoint and endpoints. Section lines across portions of the SAF were resurveyed in 1893 by J. M. Gore. We projected changes in line length onto the fault zone to measure displacement. The measurements indicate right lateral displacement of 16.2 ± 6.0 m across the fault zone. The resulting tectonic displacement exceeds the maximum reported geomorphic offsets (~6.7 m) attributed to the 1857 earthquake along the Cholame segment. Although we recognize great uncertainties in the accuracy of our small, historical data set, we tentatively conclude that total displacement in the 1857 earthquake along the SAF over this ~2 km wide aperture was significantly greater than the 3- to 6-m slip previously reported for the Cholame segment from narrower aperture geomorphic and trenching studies. These differences may be compatible if slip along the fault increases down dip rapidly from ~3–6 m at the surface to ~20 m within several hundred meters of the surface. Our inference of high slip along this portion of the Cholame segment in 1857 is at odds with most rupture models of the central SAF and suggests that geomorphic offsets may not represent total displacement across the fault zone.

Introduction

The Cholame segment of the San Andreas fault (SAF) is located between California Highway 58 in the northern Carrizo Plain and California Highway 46 at Cholame (Fig. 1) (Working Group on California Earthquake Probabilities [WGCEP], 1988). The southern segment boundary is defined by an apparent increase in the magnitude of geomorphic offsets attributed to the 1857 earthquake in the Carrizo Plain, as reported by Sieh (1978). Interpretation of geomorphic offsets in the Carrizo Plain is ambiguous (Grant and Sieh, 1993). Offsets along the Cholame segment have been interpreted to average either 3–4 m (Sieh, 1978; Sieh and Jahns, 1984) or approximately 6 m (Lienkaemper and Sturm, 1989; Lienkaemper, 2001). Hand excavations of alluvial sediments across the fault trace reveal approximately 3-m displacement from the most recent one or two earthquakes at the LY4 site (see Fig. 1), (Young *et al.*, 2001, 2002).

The different measurements and interpretations of slip yield significantly different estimates of earthquake recurrence and rupture potential for the Cholame segment (WGCEP, 1988; Arrowsmith *et al.*, 1997; Lienkaemper, 2001). In addition, paleoseismic studies in the Carrizo Plain have raised questions about rupture models that can be better tested if data are obtained for the Cholame segment (Sieh and Jahns, 1984; Grant and Sieh, 1994; Liu *et al.*, 2001). Hilley *et al.* (2001) inferred that the observed offset gradient at the Cholame–Carrizo segment boundary requires a 2/3–1/4 strength ratio of the Cholame to the Carrizo fault surfaces. More information, with particular regard to the broader deformation field and deeper slip along the fault surface, as well as independent information about the 1857 slip, will be valuable in the further characterization of the Cholame segment. Recent attempts to characterize the earthquake potential of the Cholame segment have emphasized the need for better paleoseismic, geomorphic offset, and historical land survey data (Arrowsmith *et al.*, 1997; Lienkaemper, 2001; Stone *et al.*, 2002; Southern California Earthquake Center Working Group [SCECWG], 1994; Young *et al.*, 2002).

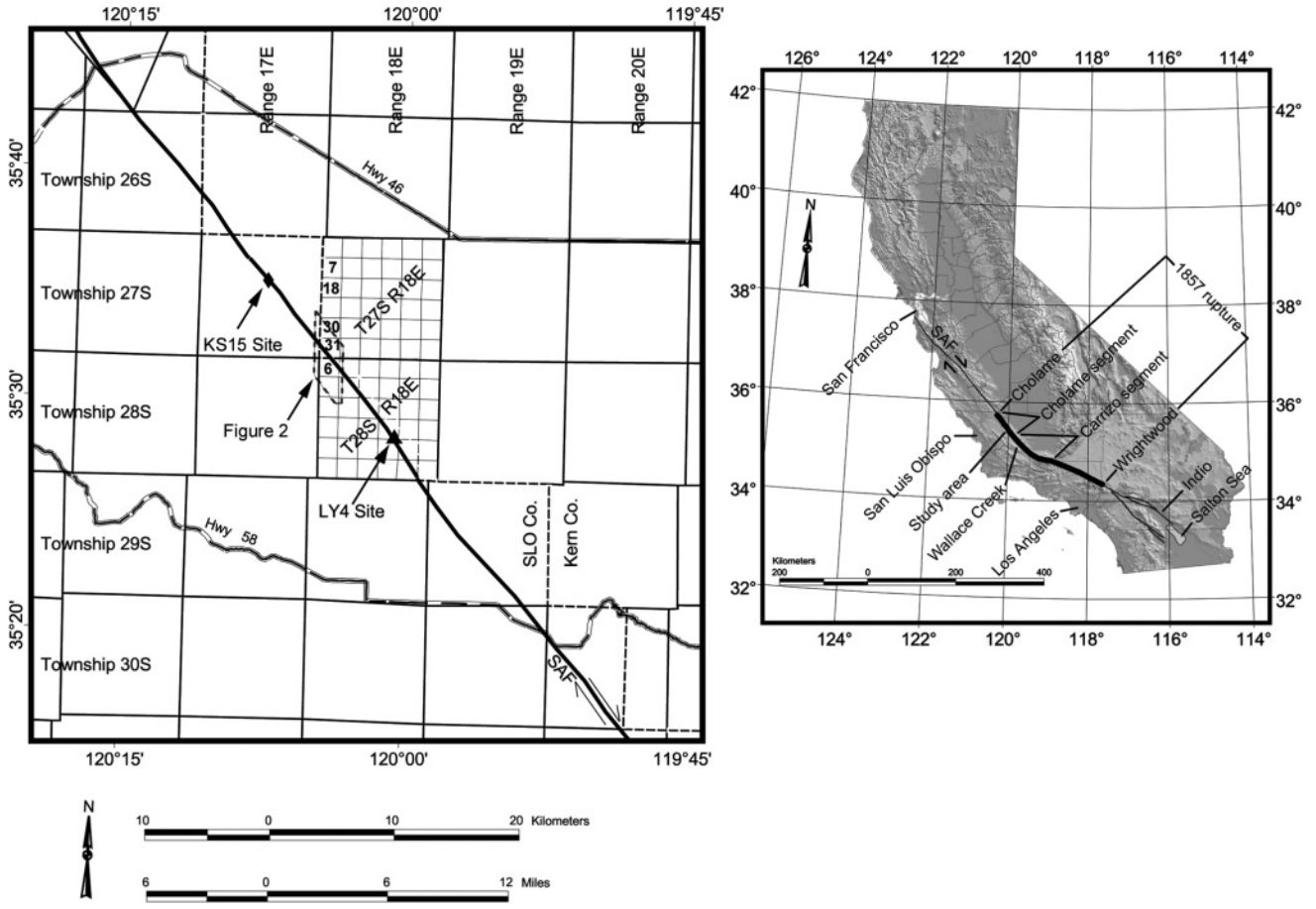

Figure 1. Location map showing California, SAF, Cholame segment, Carrizo segment, 1857 rupture extent from Cholame to Wrightwood (Sieh, 1978), and study area. Inset of study area shows SAF Cholame segment, county line (dashed line), townships, ranges, and the location of the LY4 paleoseismic excavation site (see triangle) of Stone *et al.* (2002) and 3D excavation of Young *et al.* (2001, 2002). KS15 site is the location of Kerry Sieh's site 15 discussed in Sieh (1978), Lienkaemper and Sturm (1989), and Lienkaemper (2001). Measurements listed in Table 1 were taken from sections 7, 18, 30, 31, and 6, which were surveyed by Freeman prior to the 1857 earthquake and resurveyed by Gore in 1893. Wallace Creek and the Grant and Donnellan (1994) study area are approximately 10 km southeast of California Highway 58. The Phelan fan site is ~2.6 km southeast of Wallace Creek (Grant and Sieh, 1993).

Our analysis of historical survey data provides independent measurements of displacement from the 1857 earthquake, assuming that changes reflected in the data are due to the 1857 earthquake. The surveys provide unbiased measurements because the surveyors were not aware of the significance of the SAF and the effect of tectonic displacement on survey lines.

Historical survey data have been analyzed in a similar study along adjacent segments of the SAF. Grant and Donnellan (1994) recovered two of J. E. Freeman's original monuments spanning the SAF in the Carrizo Plain, southeast of California Highway 58. By measuring the distance between the monuments and comparing it with the pre-1857 distance, they calculated 11.0 ± 2.5 m of right-lateral displacement from the 1857 earthquake near Wallace Creek (Fig. 1).

Our analysis indicates that displacement from the 1857 earthquake was 16.2 ± 6.0 m across the fault zone in this area, significantly higher than the greatest reported slip from shorter aperture geomorphic measurements. In this article, we briefly describe the rectangular survey system, our method for analyzing the surveys, the results of surveys, uncertainty in measurements, and calculations of tectonic displacement from changes in survey lines.

Review of the Rectangular Survey System

The purpose of the rectangular survey system was to establish a permanent legal system for measuring and identifying lands in the new western states (White, 1983). These surveys required a level of precision that is, coincidentally, able to estimate coseismic fault displacement. During 1855–

1893, surveyors used chains made of links to measure distances. Original surveys and resurveys in the 1800s recorded distances measured to the nearest link. One link is 7.92 in. (0.2012 m). One hundred links is one chain (66 ft, 20.117 m). Eighty chains is one mile (5280 ft, 1609.36 m). Government surveyors measured 1-mile and 0.5-mile section lines to establish endpoint and midpoint monuments. Many original monuments were constructed of wooden posts set in mounds of dirt or stone overlying a pint of charcoal. Newer and replacement monuments were made of notched stone or steel pipe with a scribed brass cap. Changes in the locations of these monuments were our basis for estimating tectonic displacement.

"The first step in the survey of an area is to divide it into tracts approximately 24 miles square by means of meridians and parallels of latitude. The 24-mile tracts are then divided into 16 townships, which are approximately 6 miles on a side. The last step, so far as the federal government is concerned, is to divide the township into 36 sections, each approximately 1 mile square" (Moffitt and Bossler, 1998, p. 629). Meridians run north and south. Baselines run east and west. Early historical cadastral survey teams relied on a compass and chains to divide land areas into sections. The methods are described more fully by White (1983), Grant and Donnellan (1994), *The 1855 Manual of Surveying Instructions* (published by U.S. Government and reprinted by White, [1983]), and Uzes (1977).

"Fraudulent surveys of the U.S. public domain are a significant factor to be considered in California retracement practice. . . . Since U.S. land surveys did not begin in California until 1851, defective work of this period was not a significant item in this state's early history. As a result of reports reaching the Commissioner of the General Land Office in Washington, D.C., about the growing trend of substandard work, field examiners were sent out in the mid-1850s to check work recently done" (Uzes, 1977, p. 174). This information in combination with a sworn statement to conform with surveying instructions suggests that Freeman's original surveys in the mid 1850s were executed faithfully.

Field notes and plats of original surveys were transcribed by the General Land Office. These transcriptions were archived on microfiche by the Cadastral Survey Office of the U.S. Bureau of Land Management (BLM). Government surveys established the legal definition of property and have been referenced in nearly all subsequent surveys by licensed surveyors. A review of BLM survey records indicated that Freeman surveyed section lines across the San Andreas Rift Zone in 1855–1856. He established monuments in Townships 26–30 south of Mount Diablo baseline. At least 26 section lines were established across the SAF between California Highways 46 and 58 prior to the 1857 Fort Tejon earthquake (Fig. 1). A subset of these section lines were resurveyed in 1893 by J. M. Gore. During resurveys, the condition of monuments and the distances between them are recorded. Records of resurveys are filed with the BLM, the Kern County Surveyor, and the San Luis Obispo County Surveyor.

Accuracy and Precision of Chained Surveys

Freeman's original surveys were conducted with a compass, chains, and poles according to rules published in the *1855 Manual of Surveying Instructions* (White, 1983). The chains were held taut, and a hand level was used to keep them horizontal. The accuracy of a chained survey depended on the skill of the surveying party, the condition of the equipment, and the terrain. The accuracy can be estimated by comparing with results of resurveys using modern equipment, assuming that monuments have not moved over time due to natural or anthropogenic causes. Grant and Donnellan (1994) calculated combined errors of one part in 950 for Freeman's surveys in the relatively flat Carrizo Plain and adjacent portions of the more rugged Temblor Range. The terrain along the Cholame segment is more rugged than in the Carrizo Plain but less rugged than the Temblor Range.

Methods

Objective

Our objective was to estimate SAF displacement from the 1857 earthquake by analyzing changes in the length of section lines that cross the fault. Changes in length were calculated to be the difference between pre-1857 survey and post-1857 survey, after calibrating for scale differences. Line-length changes were converted to total displacement and fault-parallel displacement.

Selection of Monuments and Lines for Analysis

We identified two townships (T27S, R18E, Mount Diablo Meridian [MDM], and T28S, R18E, MDM) for analysis based on their coverage of the mapped fault trace (Vedder and Wallace, 1970; Stone, 1999), having been surveyed before and after 1857, and our access to historical survey data (Fig. 1). For each township we relied on historical survey data to identify section lines that were established prior to and resurveyed within a few decades after the 1857 earthquake.

The accuracy of section-line data was evaluated using descriptions of authenticity and terrain in the records of the official resurveys. We reviewed all available survey records from 1855–1897 for each monument established in the two townships prior to 1857 (see Figs. 1, 2), classified the authenticity of monuments, and compared Freeman's original survey with Gore's resurveyed measurements of the same lines in 1893. The accuracy of section-line measurements depended, in part, on the preservation of the monuments that designated their endpoints because some monuments were reported as "lost" after the 1857 earthquake.

Monuments were classified in one of three ways: original, reestablished, or reset. Original monuments are those that remained undisturbed in their original location. Re-

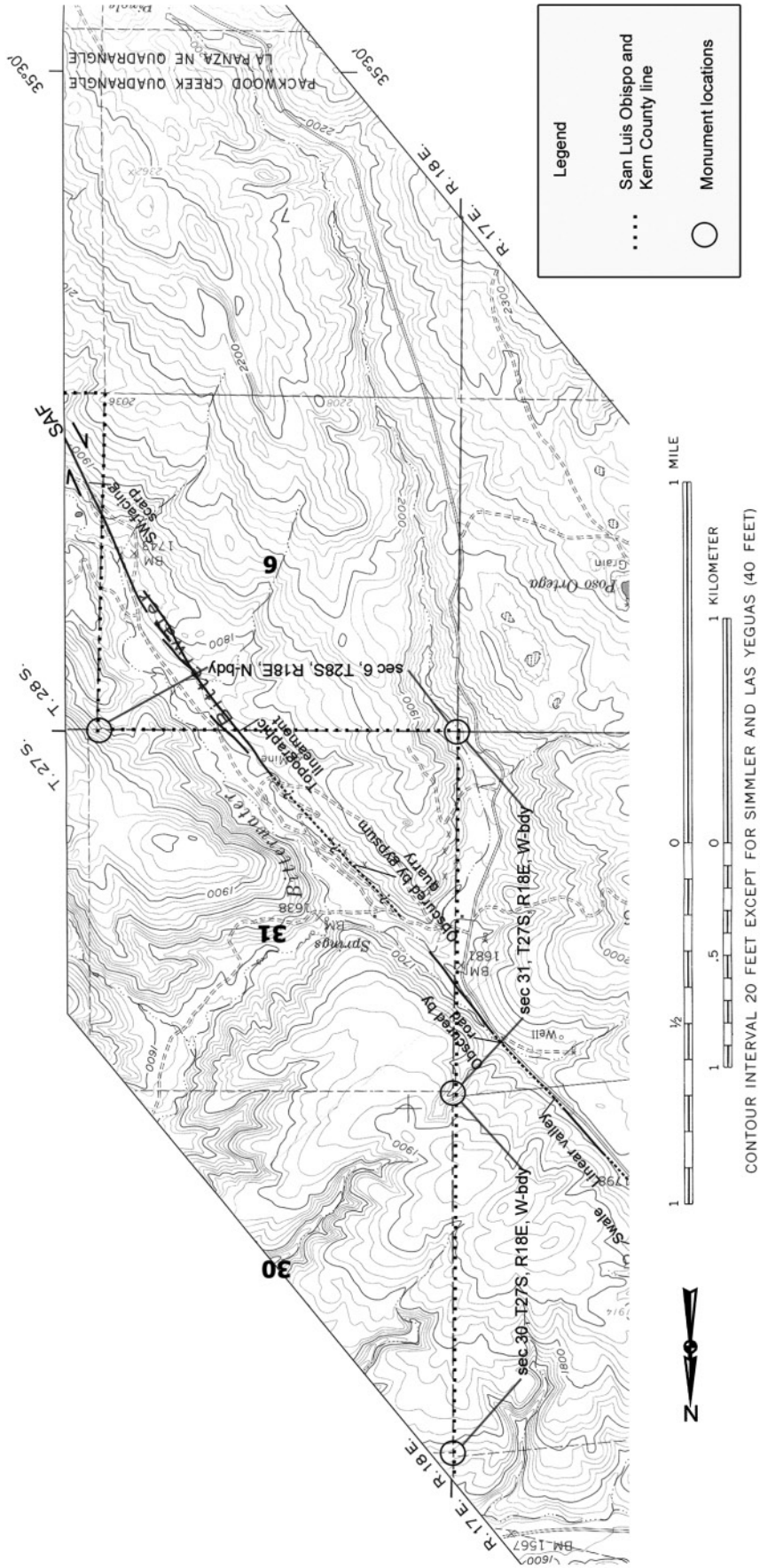

Figure 2. Map of topography and fault traces along the central portion of the Cholame segment, adapted from Vedder and Wallace (1970). This shows locations of section lines and monuments used in our analysis, except for sections 7 and 18 in T27S, R18E of the Mount Diablo Meridian (MDM), which are 1–3 miles north of section 30 and not mapped by the Vedder and Wallace (1970) map. The five monuments that mark the endpoints of the mapped section lines are circled. Section 6 is in T28S, R18E, MDM. Sections 30 and 31 are in T27S, R18E, MDM. Figure 1 shows the location of these sections with reference to California Highway 46 to the north, California Highway 58 to the south, and the county line between San Luis Obispo and Kern Counties.

established monuments are replacements of decaying or damaged monuments that were reestablished in the original location. Reset monuments replace those that were lost and later reset proportionally according to other nearby monuments. Our analysis included only section lines measured between original or reestablished monuments. Section lines designated by reset monuments were excluded because the length of these lines may have changed as a result of resetting the monuments in nonoriginal locations.

The section lines were compared to a 1:24,000-scale fault map (Vedder and Wallace, 1970) (Fig. 2) of the area in order to classify the lines as either fault crossing or non–fault crossing.

Measurement of Changes in Survey Lines

We used measurements from the original survey and the resurvey to estimate the displacement of original and reestablished monuments after the 1857 earthquake relative to monuments across the fault trace. These changes in relative position are reflected in changes from the original length of fault-crossing section lines. For a right-lateral offset along a fault striking northwest to southeast, we expect east–west fault-crossing lines to lengthen and north–south fault-crossing lines to shorten.

Errors in the survey data may be partitioned into random and systematic errors. Other elements of uncertainty are addressed in the results section. For Freeman, we adopted errors of one part in 950 (0.105%), as reported by Grant and Donnellan (1994), to account for random errors in survey measurements. For Gore, we determined the random error to be one part in 615 (0.16%), which is based on the largest variation between Gore, after calibration, and Freeman for a non-fault-crossing line (see Table 1, section 18, T27S, R18E). Systematic errors in the survey data were assessed by considering issues of accuracy and precision. To avoid confusion, we distinguish between accuracy and precision by paraphrasing Moffitt and Bossler (1998, p. 12): The accuracy of a measurement indicates how close the measurement is to the true value. An accurate measurement requires a measuring instrument that has been calibrated to a standard. The precision of a measurement indicates the degree to which the measuring instrument is able to make repeated measures of the same thing and the finest count of the measuring instrument.

If a measuring instrument demonstrates a high degree of precision but is inaccurate due to a systematic error, then calibration may be all that is necessary to have a useful instrument. When we compare the measurements of the non-fault-crossing lines within each survey (Table 1), we find them to be internally consistent. Therefore, the differences between the two surveys may be reconciled by accounting for systematic scale error.

A scale factor was used to adjust for systematic scale error between the surveys. We calibrated Gore's measurements by using Freeman's measurements of non-fault-crossing lines (Table 1). A scale factor of 0.9892 was calculated by finding the mean of quotients that resulted from Freeman's measurement divided by Gore's measurement for each non-fault-crossing line. Multiplying Gore's reported measurements by the scale factor calibrated the surveys so that differences between them are more accurate. Table 1 shows the measurements that the surveyors reported and our calibration of Gore's 1893 measurements.

Two assumptions are necessary for using a scale factor to calibrate Gore's measurements to Freeman. First, the measurements reported by each survey must be precise. Even though the measurements of the same line between surveys may vary due to differences in instruments, a survey's repeated measurements of a given line should be the same, after accounting for random error. Second, the actual length of non-fault-crossing lines must not have changed during the time period between the surveys; otherwise, calibration by the scale factor would be invalid.

Monument displacement is represented by changes in

Table 1
Surveyors' Measurements and Monuments' Displacement

	1855: Freeman	1893: Gore		Difference between Gore (cal) and Freeman
Section Line	Reported in Chains	Reported in Chains	Calibrated by Us in Chains	Chains
Fault-Crossing Lines				
N-bdy, sect 6, T28S, R18E	80.00	81.21	80.33	+0.33
W-bdy, sect 31, T27S, R18E	80.00	80.08	79.22	−0.78
Non-Fault-Crossing Lines				
W-bdy, sect 7, T27S, R18E	80.00	80.75	79.88	−0.12
W-bdy, sect 18, T27S, R18E	80.00	81.00	80.13	+0.13
W-bdy, sect 30, T27S, R18E	80.00	80.87	80.00	0.00

Gore is calibrated to Freeman using the non-fault-crossing lines to find the scale factor of 0.9892 = [(80/80.75) + (80/81.00) + (80/80.87)]/3. Measurements reported in surveys by Freeman in 1855–1856 and Gore in 1893, our calibration of Gore's survey measurements, and the difference between Freeman's measurement and Gore's calibrated measurement for each line. The change in length of fault-crossing line N-bdy, sect 6, T28S, R18E, was used to find dE. The change in length of fault-crossing line W-bdy, sect 31, T27S, R18E, was used to find dN. All units in chains. 1 chain = 66 ft = 20.117 m. Abbreviations: n, north; s, south; e, east; w, west; bdy, boundary; T, township; R, range; sect, section.

length of fault-crossing lines between the pre-1857 survey by Freeman and the post-1857 survey by Gore. We refer to displacement in the east–west direction as dE and in the north–south direction as dN. We converted from a reported measurement of χ chains to L, in meters, using

$$L = (\chi \text{ chains})(20.117 \text{ m per chain}). \quad (1)$$

The small size of our sample limits the usefulness of statistical methods for assessing error. To account for error, we calculated fault displacement using a range of values for dE and dN. Based on reported measurements and rates of random error, we find that the actual length L, in meters, of χ chains may range between minimum, L_{min}, and maximum, L_{max}, values as follows: $L_{min} \leq L \leq L_{max}$, where

$$L_{min} = [L - (L)(\text{error } \%)], \text{ and } L_{max} = [L + (L)(\text{error } \%)]. \quad (2)$$

For example, the actual length of a reported measurement of 80.00 chains, given Freeman's random error of 0.105%, is between $L_{min} = 1607.7$ m and $L_{max} = 1611.1$ m. Similarly, the actual length of a reported measurement of 80.00 chains, given Gore's random error of 0.16%, is between $L_{min} = 1606.8$ m and $L_{max} = 1612.0$ m.

The range of values for possible actual lengths of section lines was used to find the range of values for the amount of monument displacement. Given a fault-crossing line trending in the east–west direction,

$$\text{dE} = (L_{\text{Gore}} \pm 0.16\%) - (L_{\text{Freeman}} \pm 0.105\%), \quad (3)$$

where L_{Gore} is the length measured by Gore in 1893, but calibrated by us, and L_{Freeman} is the length measured by Freeman in 1855–1856. Likewise, for a fault-crossing line trending in the north–south direction,

$$\text{dN} = (L_{\text{Gore}} \pm 0.16\%) - (L_{\text{Freeman}} \pm 0.105\%). \quad (4)$$

Calculation of Displacement and Fault Slip

Total displacement (**dU**) across the fault zone in the area of the survey lines was calculated from dE and dN using the Pythagorean theorem:

$$\mathbf{dU} = (\text{dE}^2 + \text{dN}^2)^{1/2}. \quad (5)$$

The total displacement vector was then projected onto the fault to estimate fault slip, dS, and fault-normal component, N, during the period between surveys. Figure 3 illustrates the relationships between SAF, dE, dN, **dU**, dS, N, and angles δ, α, and γ. Angle δ is formed between the north–south line, dN, and the displacement vector, **dU**. Angle α is formed between the displacement vector, **dU**, and the fault slip, dS. Angle γ is the SAF strike. The azimuth of **dU** (δ) is found using the equation:

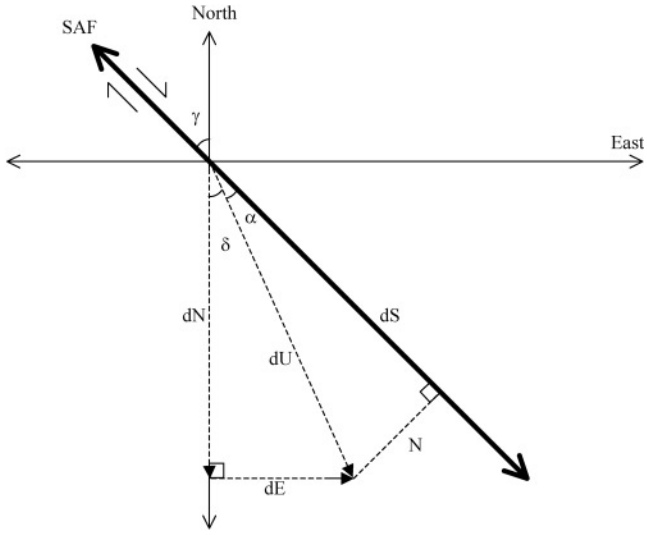

Figure 3. Diagram showing the relationships among SAF, dE, dN, **dU**, dS, and N, and angles δ, α, and γ in order to calculate fault slip from monument displacement vectors. The change in length of the east–west section line is marked as dE. The change in length of north–south section line is marked as dN. The total displacement vector is **dU**. Fault-parallel slip is dS. The fault normal component is N. Angles δ is the azimuth of the total displacement vector. Angle γ is the strike of SAF. Angle α is the difference between the SAF strike and δ.

$$\delta = \arctan(\text{dE/dN}). \quad (6)$$

Angle γ represents the strike of SAF. Therefore, $\alpha = \gamma - \delta$. A right triangle is formed with legs dS and N, hypotenuse **dU**, and interior angle α. Using trigonometry we find

$$\text{dS} = \mathbf{dU} \sin(90 - \alpha) \quad (7)$$

and

$$N = \mathbf{dU} \sin \alpha. \quad (8)$$

Total displacement and fault slip were estimated from displacement of the monuments, as described in data and results. Postseismic and interseismic displacement of the monuments was also modeled to evaluate their magnitude and significance. Over the time interval of survey measurements, noncoseismic displacements are negligible. If the models are extended to the present, there is a maximum displacement of approximately 20 cm along the survey lines. The displacement between 1855 and 1893 is negligible.

Data and Results

The reported survey measurements, calibrated measurements, and resulting monument displacements are shown in Table 1. Values for dE, dN, **dU**, dS, N, and angles δ, α, and

γ are listed in Table 2. Figure 3 illustrates the relationships between SAF, dE, dN, **dU**, dS, *N*, and angles δ, α, and γ.

The Vedder and Wallace (1970) fault map shows that in townships T27S R18E MDM and T28S R18E MDM there are 13 SAF-crossing lines. Of these 13 lines, 10 were surveyed prior to 1857 by Freeman, and 2 of these were resurveyed by Gore using Freeman's original monuments (Fig. 2). We also identified three non-fault-crossing lines that were resurveyed by Gore using Freeman's monuments.

Monument Displacement from Line Length Changes

Values for dE are based on comparing the reported measurements from Freeman's 1855 survey to Gore's 1893 survey of the north boundary for section 6, T28S, R18E. After calibration, we find Gore's measurement to be 0.33 chains longer than Freeman's measurement. The line lengthened during the time between the surveys by 6.6 $\pm$ 4.3 m.

Values for dN are based on comparing the reported measurements from Freeman's 1855 survey to Gore's 1893 survey of the west boundary for section 31, T27S, R18E. After calibration, we find Gore's measurement to be 0.78 chains shorter than Freeman's measurement. The line shortened during the time between the surveys by 15.7 $\pm$ 4.2 m.

The combination of the values used for dE and dN affects the values of interior angles δ and α, which, in turn, affects fault slip, dS. The value for angle α depends on the SAF strike (γ) and angle δ. In the study region the fault strike (γ) varies locally between 40°–50° west of north, but the prevailing strike is N40°W (Vedder and Wallace, 1970) (Fig. 2). We used five combinations of the minimum, maximum, and average values of dE and dN to determine the value for dS, *N*, and the corresponding range due to random errors (Table 2). Using the average north and east components (dN = 15.7 m and dE = 6.6 m, respectively), we calculated $\delta = 22.8°$. Therefore, because $\gamma = 40°$, $\alpha = 17.2°$. Logically, the value for δ will decrease as the difference between dN and dE increases. As δ decreases, α increases, which affects the value for fault slip.

Total Displacement and Fault Slip from Monument Displacement

The displacement of the monuments, dE and dN, are components of the total displacement vector (**dU**), as shown in Figure 3. Based on the average monument displacement values for dE and dN, we find that **dU** = 17.0 m (Table 2). Using the minimum values for monument displacement, **dU** = 11.7 m. Using the maximum values for monument displacement, **dU** = 22.7 m. Given the values for **dU** and corresponding α, fault slip (dS) is 16.2 $\pm$ 6.0 m. The fault-normal component of displacement (*N*) is 5.0 $\pm$ 6.0 m. For almost all combinations of values for dE and dN, the fault-normal component indicates a compressional component of motion along the fault. A small set of combinations of values for dE and dN indicates pure strike-slip motion along the fault (11.5 m $\leq$ dN $\leq$ 13.0 m, dE = dN $\times$ tan 40, $N \approx 0$, 15.0 m $\leq$ dS $\leq$ 17.0 m). For a smaller set of combinations of values for dE and dN, the fault-normal component indicates a tensional component of motion along the fault (11.5 m $\leq$ dN $\leq$ 12.5 m, 10.0 $\leq$ dE $\leq$ 10.9, and $\delta > 40°$, N < 0, 15.8 m $\leq$ dS $\leq$ 16.6 m).

Interseismic and Postseismic Strain Accumulation

To estimate the contribution of interseismic motion to the fault-parallel displacement we determined the displacement field at the surface from a horizontal screw dislocation buried at depth *D* in the lithosphere. Interseismic motion is modeled as slip from the base of the depth of coseismic faulting (also *D*) to negative infinity; whereas, coseismic motion is modeled as slip confined to the upper portion of the fault from the surface to a depth of *D* (Thatcher, 1990). For a 2-km-wide fault-normal aperture (spanning all measurements in this study), the 38 years between the 1855 Freeman and 1893 Gore surveys would accumulate a 6-cm displacement discontinuity assuming 35 mm/yr average slip rate and deep slip below 15 km. The calculations of interseismic displacement assume a constant interseismic strain rate

Table 2
Values Used to Calculate Range of Fault Slip Values from Monument Displacement

	Displacement Variables							
Monument Displacement	dE (m)	dN (m)	**dU** (m)	$\gamma°$	$\delta°$	$\alpha°$	dS (m)	*N* (m)
dE_{min}, dN_{min}; minimum dS	2.3	11.5	11.7	40.0	11.3	28.7	10.3	5.6
dE_{max}, dN_{min}; minimum N	10.9	11.5	15.8	40.0	43.5	−3.5	15.8	−1.0
dE_{ave}, dN_{ave}; average dS, N	6.6	15.7	17.0	40.0	22.8	17.2	16.2	5.0
dE_{min}, dN_{max}; maximum N	2.3	19.9	20.0	40.0	6.6	33.4	16.7	11.0
dE_{max}, dN_{max}; maximum dS	10.9	19.9	22.7	40.0	28.7	11.3	22.3	4.4

Values used to calculate fault slip from monument displacement: monument displacement in the east–west direction, dE; monument displacement in the north–south direction, dN; total displacement, $\mathbf{dU} = (dE^2 + dN^2)^{1/2}$; fault parallel slip, $dS = \mathbf{dU} \sin(90 - \alpha)$; fault-normal component, $N = \mathbf{dU} \sin \alpha$; SAF strike, $\gamma = 40°$; azimuth of total displacement, $\delta = \arctan(dE/dN)$; angle between the displacement vector and the fault slip, $\alpha = \gamma - \delta$. When accounting for error, dE and dN each have minimum, average, and maximum values that are used to find the range of possible values for dS and *N*.

since 1857. However, these results are minimum because of the observation of a higher postseismic strain transient, which has been shown to decrease exponentially with time until reaching the interseismic rate after large earthquakes (Thatcher, 1983). In order to correct for this increased amount of postseismic displacement, we empirically determined the exponential decay of shear strain rate based on data from Thatcher (1983) and integrated over the elapsed time from 1857 to the measurements to get the accumulated total shear strain. Multiplying the total strain by the aperture of the two points perpendicular to the SAF (2 km) yielded a total postseismic displacement of about 10 cm. Thus, given the relatively short temporal (38 years) and spatial (<2 km perpendicular to the fault) apertures of measurement, interseismic and postseismic contributions to the displacement are less than about 20 cm (e.g., Thatcher, 1983, 1990), and so we assume they are negligible.

Uncertainty within Data and Results

Not all elements of uncertainty can be controlled in this study. Core uncertainties arise from issues of monument location and the accuracy of records of measurements between monuments. Monument location could be affected by landsliding, nontectonic creep, proportional resets, or human meddling.

Landslides and indicators of soil creep are recognizable on slopes in the Cholame segment region, including our study area. For example, a closed depression 0.5 km southwest of the southwest corner of section 31, T27S, R18E, was probably formed by a landslide (Fig. 2). The monument does not appear to be located on the landslide, and Gore's description of the monument in 1893 suggests that it was not disturbed during the 38-year period since it was established. Other monuments clearly were disturbed and are, therefore, excluded from our study. However, we cannot rule out displacement of monuments by unrecognized slope movement. Slope creep and recent landsliding may be difficult to identify in the area (Lienkaemper and Sturm, 1989; Stone *et al.*, 2002; Young *et al.*, 2002).

The accuracy and precision of the surveyor's ability to measure distances was probably influenced by the characteristics of the terrain, such as steepness and vegetation. The descriptions provided by Freeman and Gore of the terrain that was traversed for the five lines in our study are similar, being somewhat mountainous with little vegetation. The accuracy of the records of the measurements depends on the accuracy and legibility of the surveyor's notes of those measurements and the accuracy of clerk who transcribed the surveyor's notes into the official typed record on file.

The general results from the data are kinematically consistent: the east–west fault-crossing line lengthened and the north–south fault-crossing line shortened during the period between the surveys. After calibrating to correct for scale differences, the lengths of non-fault-crossing lines are consistent, within a known error, between the surveys.

Discussion

The principal purpose of our study is to measure the total displacement from the 1857 earthquake and compare it with reported slip from measurements of geomorphic offsets. Our results indicate that slip along the Cholame segment may have been greater than 3 m previously reported from narrower aperture geomorphic (Sieh, 1978) and trenching studies (Young *et al.*, 2002). Analysis of the surveys also shows that total displacement exceeded the maximum reported geomorphic offsets (e.g., ~6.7 m by Lienkaemper [2001]). This is not surprising given the significantly greater aperture of measurement for the survey lines.

The earthquake potential of the Cholame segment has been debated since Sieh and Jahns (1984) and Harris and Archuleta (1988) forecast a *M* 7 Parkfield–Cholame earthquake based, in part, on Sieh's (1978) and Sieh and Jahns's (1984) reports of 3–4m slip on the Cholame segment in the 1857 earthquake. The amount of slip was inferred from measurements of geomorphic offsets. More recently, Lienkaemper and Sturm (1989) and Lienkaemper (2001) analyzed geomorphic offsets along the same section of the fault and concluded that the slip ranged from 5.4 to 6.7 m.

The different slip values reported for the Cholame segment highlight the uncertainty inherent in the method of estimating slip from measurements of offset geomorphic features. Grant and Sieh (1993) presented two rupture scenarios for recent earthquakes in the Carrizo Plain based on variations in measurements of offset streams along the SAF. McGill and Rubin (1999) demonstrated that geomorphic offsets along the 1992 Landers earthquake rupture zone could be misinterpreted as evidence for multiple earthquakes based on geomorphic analysis alone. In general, interpretation of slip from geomorphic offsets is ambiguous because the number of earthquakes that generated each offset is uncertain (Grant, 2002).

An alternative method of measuring paleoslip is to conduct a 3D excavation to identify the number of ruptures that contributed to each offset and to concurrently date each surface rupture. Grant and Sieh (1993) measured approximately 6.7 m of dextral offset along the SAF at Phelan fan using 3D excavation. Their results agree well with measurements of offset streams near the excavation site, but offset streams 2–3 km to the northwest near Wallace Creek average approximately 9.5 m (Sieh and Jahns, 1984).

The difference in interpreted slip could be due to different aperture of measurement (shorter for the 3D excavation) or variation in slip along the fault, or both. Grant and Donnellan (1994) attempted to resolve the discrepancy by measuring 1857 slip from pre- and post-1857 surveys across the fault between Wallace Creek and the Phelan fan (Fig. 1). They reported approximately 11 m of slip distributed across a 1-mile section line, consistent with geomorphic measurements at Wallace Creek, but the uncertainty in their measurements are too great to rule out the possibility of 6.7-m

total slip across the fault at the Phelan fan. In general, measurements of 1857 slip across the SAF in the Carrizo Plain appear to show greater displacement with larger measurement aperture, suggesting that there is some off-fault deformation. Measurements of cultural features displaced by the North Anatolian fault zone during the 1999 Izmit earthquake reveal a significant amount of deformation beyond the geomorphically visible fault trace (Rockwell *et al.*, 2001).

Results of fault displacement calculations present the possibility that slip across the entire fault zone in the 1857 earthquake was significantly greater than slip interpreted from the greatest geomorphic offsets in a narrow zone along the fault trace. If so, this result implies that total slip for the Cholame segment was greater and the recurrence time for comparable earthquakes may be longer than previously suspected. This interpretation is consistent with the results of paleoseismic excavations at the LY4 site, which is ~8.5 km southeast of our study area (Fig. 1). Stone *et al.* (2002) reported fewer surface ruptures and longer average recurrence times relative to ruptures in the Carrizo Plain, Pallett Creek, and Wrightwood. Recent work by Young *et al.* (2001, 2002) appears to confirm the longer recurrence intervals for Cholame segment ruptures.

A simple exploration of these data using the dislocation theory presented earlier for the analysis of interseismic data (Thatcher, 1990) can reconcile both data sets (Fig. 4). In this analysis, we use one pair of dislocations to simulate shallow slip along the SAF of 3 m, such as what is inferred by Young *et al.* (2001). We use a second pair to represent the deeper slip that will have driven the displacements farther from the fault trace. There is a tradeoff between deep-slip magnitude and depth to the top of the deeper slip-patch. However, if we assume a 20-m deep slip and 3 m at the surface, then the displacements we infer here are consistent with a depth of transition up to about 0.5 km. Figure 4 shows a block diagram of the idealized 2D fault zone and the geometry of the abrupt transition in slip magnitude. In reality, this transition could be more gradual or may coincide with the base of the Paso Robles formation. The calculated displacement pattern satisfies the 3-m offset in the very near field (trench). Shallow transition depths to 20 m slip will also displace the monuments by almost 20 m. This illustration implies that if both data sets characterize what happened in 1857, significant distributed deformation must have occurred in the fault zone away from the most active trace. Mapping by Vedder and Wallace (1970), Stone (1999), and Young *et al.* (2001) do not show any other major surface-rupturing structures in the area, so deformation would have to be accommodated by numerous small faults and fractures and possibly by flow in shallow materials. This provides an illustration of the

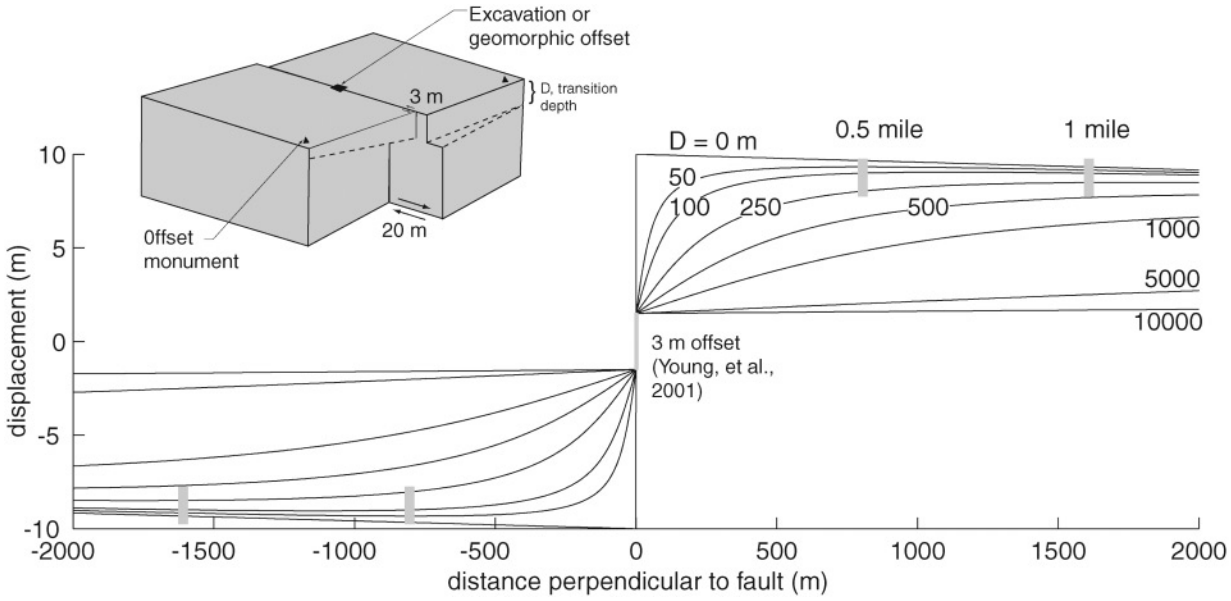

Figure 4. Paired horizontal screw dislocations simulate shallow slip of 3 m and a deeper slip of 20 m (Thatcher, 1990). Shallow transition depths will cause monuments up to 2000 m away to be displaced by much larger magnitudes than geomorphic or 3D trench studies might measure. The inset diagram shows the idealized 2D fault zone (the dislocations are infinite in the third or along-fault dimension) and relative positions of an excavation and monuments. The transition between low and high slip is probably not as abrupt as depicted. The plot shows the fault-parallel displacement as a function of distance perpendicular to the simulated fault. *D* is the depth of transition between low and high slip. The central box shows the approximated extent of offset landforms (as measured by Young *et al.*, 2001), and the gray ticks show positions of 0.5 and 1 miles from the fault trace. Monuments from this study are less than 1 mile from the fault trace.

structural geologic behavior of a fault zone in which the poorly confined and highly deformed fault zone materials do not accommodate a majority of the deeper fault slip as it propagates coseismically to the surface.

Our inference of high slip along this portion of the Cholame segment in 1857 is at odds with most models of rupture potential for the central SAF (Sieh and Jahns, 1984; Arrowsmith *et al.*, 1997; WGCEP, 1988) that assume the Cholame segment ruptures more frequently than other segments (with the exception of Parkfield). The larger amount of fault-parallel slip along the Cholame segment relative to the Carrizo segment (16.2 m versus 11.0 m of Grant and Donnellan [1994]) and the longer average recurrence time (236 years for Cholame versus 156 years for Carrizo [Stone *et al.*, 2002]) suggests the possibility that the Cholame segment may be an asperity that controls rupture of large earthquakes comparable to the 1857 event. In addition, it would imply that the Cholame segment could be stronger than the adjacent Carrizo segment, contrary to the inference from Hilley *et al.* (2001) which was based on the available surface, short aperture geomorphic offset data.

Conclusion

Measurements of line-length changes from historical surveys immediately prior to and after the 1857 earthquake show that total coseismic displacement may have been significantly greater than the greatest reported slip from measurements of geomorphic offsets and excavations in the fault zone. The discrepancies in measurements may be a result of measurement aperture, with larger total displacement measured across greater distances spanning the fault zone. Displacement exceeding 6 m is consistent with reported long recurrence intervals for the Cholame segment.

Acknowledgments

The authors thank Roland Bürgmann for reviewing our displacement calculation methods and Larry Vredenburgh from the Bureau of Land Management for pointing out the availability of the historical land survey data and for encouraging this work. Constructive criticism by J. Savage, an anonymous reviewer, and W. Lettis led to significant improvements in the manuscript. Conversations with Jeri Young and George Hilley have been helpful in the clarification of ideas presented here. This research was supported by the Southern California Earthquake Center (SCEC). SCEC is funded by National Science Foundation Cooperative Agreement EAR-8920136 and U.S. Geological Survey Cooperative Agreements 14-08-0001-A0899 and 1434-HQ-97AG01718. The SCEC Contribution Number for this article is 586. Partial support was provided by a University of California–Irvine award to L. B. Grant. This is Department of Environmental Analysis and Design Contribution Number 8.

References

Arrowsmith, J R., K. McNally, and J. Davis (1997). Potential for earthquake rupture and M7 earthquakes along the Parkfield, Cholame, and Carrizo segments of the San Andreas Fault, *Seism. Res. Lett.* **68,** 902–916.

Grant, L. B. (2002). Paleoseismology, in *IASPEI Handbook of Earthquake and Engineering Seismology*, W. H. K. Lee, H. Kanamori, P. C. Jennings, and C. Kissinger (Editors), Academic Press, New York.

Grant, L. B., and A. Donnellan (1994). 1855 and 1991 Surveys of the San Andreas fault: implications for fault mechanics, *Bull. Seism. Soc. Am.* **84,** 241–246.

Grant, L. B., and K. Sieh (1993). Stratigraphic evidence for 7 meters of dextral slip on the San Andreas fault during the Great 1857 earthquake in the Carrizo Plain, *Bull. Seism. Soc. Am.* **83,** 619–635.

Grant, L. B., and K. Sieh (1994). Paleoseismic evidence of clustered earthquakes on the San Andreas fault in the Carrizo Plain, California, *J. Geophy. Res.* **99,** 6819–6841.

Harris, R. A., and R. J. Archuleta (1988). Slip budget and potential for a M7 earthquake in central California, *Geophy. Res. Lett.* **15,** 1215–1218.

Hilley, G. E., J R., Arrowsmith, and E. Stone (2001). Inferring segment strength contrasts and boundaries along low-friction faults using surface offset data, with an example from the Cholame-Carrizo segment boundary along the San Andreas Fault, Southern California, *Bull. Seism. Soc. Am.* **91,** 427–440.

Lienkaemper, J. J. (2001). 1857 Slip on the San Andreas fault southeast of Cholame, California, *Bull. Seism. Soc. Am.* **91,** 1659–1672.

Lienkaemper, J. J., and T. A. Sturm (1989). Reconstruction of a channel offset in 1857(?) by the San Andreas Fault near Cholame, California, *Bull. Seism. Soc. Am.* **79,** 901–909.

Liu, J., Y. Klinger, K. Sieh, and C. Rubin (2001). 3D Excavation shows slight slip variations in recurrent ruptures of the San Andreas fault, *Seism. Res. Lett.* **72,** 266.

McGill, S. F., and C. M. Rubin (1999). Surficial slip distribution on the central Emerson fault during the June 28, 1992, Landers earthquake, California, *J. Geophys. Res.* **104,** 4811–4833.

Moffitt, F. H., and J. D. Bossler (1998). *Surveying*, Tenth ed., Addison Wesley, Menlo Park, California, 738 pp.

Rockwell, T. K., T. Dawson, S. C. Lindvall, W. Lettis, R. Langridge, and Y. Klinger (2001). Lateral offsets on surveyed cultural features resulting from the 1999 Izmit and Duzce earthquakes, Turkey, *Seism. Res. Lett.* **72,** 266.

Sieh, K. E. (1978). Slip along the San Andreas fault associated with the great 1857 earthquake, *Bull. Seism. Soc. Am.* **68,** 1421–1448.

Sieh, K. E., and R. H. Jahns (1984). Holocene activity of the San Andreas fault at Wallace Creek, California, *Geol. Soc. Am. Bull.* **95,** 883–896.

Southern California Earthquake Center Working Group (SCECWG) on the Probabilities of Future Large Earthquakes in Southern California (1994). Seismic Hazards in Southern California: probable earthquakes, 1994–2024, *Bull. Seism. Soc. Am.* **85,** 379–439.

Stone, E. M. (1999). Geomorphology, structure and paleoseismology of the central Cholame segment, Carrizo Plain, California, *M. S. Thesis*, Arizona State University, Tempe, 100 pp.

Stone, E. M., L. B. Grant, and J R. Arrowsmith (2002). Recent rupture history of the San Andreas fault southeast of Cholame in the northern Carrizo Plain, California, *Bull. Seism. Soc. Am.* **92,** no. 3, 983–997.

Thatcher, W. (1983). Nonlinear strain buildup and the earthquake cycle on the San Andreas fault, *J. Geophy. Res.* **88,** 5893–5902.

Thatcher, W. (1990). Present-day crustal movements and the mechanics of cyclic deformation, in *The San Andreas Fault System, California*, R. E. Wallace (Editor), *U.S. Geol. Surv. Prof. Pap. 1515*, 189–205.

Uzes, F. D. (1977). *Chaining the Land: A History of Surveying in California*, Landmark, Sacramento, 315 pp.

Vedder, J. G., and R. E. Wallace (1970). Map showing recently active breaks along the San Andreas and related faults between Cholame Valley and Tejon Pass, CA, U.S. Geol. Surv. Misc. Geol. Invest. Map I-574, scale 1:24,000.

White, C. A. (1983). *A History of the Rectangular Survey System*, Bureau of Land Management, U.S. Dept. of Interior, U.S. Govt. Printing Office, Washington D.C., 774 pp.

Working Group on California Earthquake Probabilities (WGCEP) (1988). Probabilities of large earthquakes occurring in California on the San Andreas Fault, *U.S. Geol. Surv. Open-File Rept. OF 88-398*, 62 pp.

Young, J. J., J R. Arrowsmith, L. Colini, L. B. Grant, and B. Gootee (2002). 3D excavation and recent rupture history along the Cholame segment of the San Andreas fault, *Bull. Seism. Soc. Am.* **92,** no. 7, 2670–2688.

Young, J. J., L. Colini, J R. Arrowsmith, and L. B. Grant (2001). Recent ruptures along the Cholame segment of the San Andreas fault, CA, *Seism. Res. Lett.* **72,** 266.

Department of Environmental Analysis and Design
University of California–Irvine
Irvine, California 92697-7070
(E.E.R., L.B.G.)

Department of Geological Sciences
Arizona State University
Tempe, Arizona 85287-1404
(J.R.A., E.M.S.)

Department of Geology and Geography
Georgia Southern University
Statesboro, Georgia 30460-8149
(D.D.R.)

Manuscript received 14 May 2001.